Nuclear Physics B329 (1990) 263–284
North-Holland

THE CORRELATION LENGTHS AND THE ORDER OF THE PHASE TRANSITION IN THREE-DIMENSIONAL Z_3 SYMMETRIC MODELS

Sourendu GUPTA, A. IRBÄCK and B. PETERSSON

Fakultät für Physik, Universität Bielefeld, Postfach 8600, D-4800 Bielefeld 1, FRG

R.V. GAVAI* and F. KARSCH

Theory Division, CERN, CH-1211 Geneva 23, Switzerland

Received 24 April 1989

We present a high statistics Monte Carlo investigation of three-dimensional Z_3 symmetric models, which are related to SU(3) pure gauge theory at finite temperature. From the finite size scaling behaviour of bulk properties and the existence of metastable states, we conclude that these models exhibit a first-order phase transition. We have also performed detailed correlation length measurements in a cylindrical geometry with periodic boundary conditions as well as with a cold wall in the longitudinal direction. The correlation length, which appears to be independent of the boundary conditions, becomes very large near the critical point. Nonetheless, our data suggest that the correlation length develops a discontinuity at the critical point in the infinite volume limit.

1. Introduction

Many numerical investigations of the phase structure of SU(3) gauge theory at finite temperature have been performed. Early studies, focusing on thermodynamic functions, gave seemingly clear evidence for the existence of a first-order phase transition (see, e.g., ref. [1]), signalled by large discontinuities in the order parameter as well as in bulk quantities like the energy density, ϵ, and entropy density, s. During the last year large-scale computations have been performed to re-examine this picture on large lattices. A detailed analysis of the entropy density, close to the critical temperature T_c, showed that the gap in the entropy density is considerably smaller than previously thought [2]. However, since the gap became more pronounced with increasing spatial lattice size, the first-order nature of the SU(3) deconfinement transition was confirmed in the same study [2]. A concurrent study of the correlation length ξ, on the other hand, yielded a linear scaling of the correlation length at T_c with the (transverse) size L of the lattice, i.e. $\xi(T_c) \sim L$

* On study leave from Tata Institute of Fundamental Research, Bombay 400005, India

0550-3213/90/$03.50

[3,4]. This suggests that $\xi(T_c)$ diverges in the infinite volume limit, which has been taken as an indication for a possible second-order phase transition.

A second-order deconfinement transition in the SU(3) gauge theory would require a new look at the universality arguments given by Svetitsky and Yaffe [5], which led to the prediction that the phase transition in SU(3) gauge theory is first-order. They argue that the effective theory for the $(3+1)$-dimensional finite temperature SU(N) gauge theory is a 3-d Z_N symmetric spin model with short range interactions, dominated by a ferromagnetic nearest neighbour coupling. Their prediction for SU(3) is based on the fact that no fixed points are known for such models with global Z_3 symmetry. Their arguments can be verified in the strong coupling limit for SU(N) gauge theories [6,7] and more recently have been checked in a detailed Monte Carlo renormalization group analysis [8] for the SU(2) gauge theory.

In the case of Z_3 symmetric models it is known that anti-ferromagnetic interactions can give rise to second-order phase transitions [9]. Recently a model with a mixture of ferromagnetic and anti-ferromagnetic couplings has been studied [10] to look for explanations of the possible failure of the universality arguments for the SU(3) gauge theory. However, before considering such alternatives, one should perhaps reconsider first in greater detail the behaviour of the correlation length and other thermodynamic observables near a first-order phase transition. The general folklore about first-order transitions is that quantities like the correlation length ξ or the specific heat, C_V, stay finite at T_c. This assumes that the critical temperature T_c is approached on an infinite lattice. However, the order of the limiting procedure is crucial here. It is known that even if the transition is of first-order, thermodynamic quantities measured on finite lattices at T_c, can diverge when the infinite volume limit is taken [11,12]. In order to distinguish a first-order from a second-order transition a detailed finite size analysis, yielding various critical exponents, is required. It thus seems important to understand the thermodynamics of Z_3 symmetric models with ferromagnetic nearest neighbour coupling and compare with the behaviour found in the SU(3) theory. Models relevant to the SU(3) theory are the 3-d three-state Potts model and the 3-d Polyakov loop model. The former has been studied in detail in a recent Monte Carlo simulation [13] in a cubic geometry. The Polyakov loop model is an effective 3-d spin model for the SU(3) theory that one obtains in the strong coupling limit by systematically integrating out all spatial degrees of freedom [6,7], and thus is, in a sense, intermediate between the Potts model and the SU(3) gauge theory.

We have analyzed the thermodynamic properties on cubic lattices with periodic boundary conditions and have performed a high statistics numerical analysis of the correlation lengths in these models on lattices with cylindrical geometry. The thermodynamic behaviour of the Polyakov loop model is found to be very similar to that of the Z_3 Potts model in three dimensions [13]. We find that the phase transition is first-order, in agreement with expectations based on universality [5] and mean field calculations [7]. In the critical region, run-time histories for the order

parameter Re(tr W) show clear metastabilities, and the associated probability distributions exhibit well-separated peaks corresponding to ordered and disordered states. The analysis of the finite size scaling behaviour of peaks in response functions, as well as critical coupling β_c^L, agrees well with the behaviour expected for first-order phase transitions. Another main aim of this paper is to study in detail the behaviour of the correlation length on asymmetric lattices with and without a cold wall. The study is intended to be very similar to the one made for SU(3) [3, 4]. On an asymmetric lattice of size $L^2 \times L_z$ with $L_z \gg L$, we measure the correlations of spin operators averaged over transverse planes. We have worked with three different lattice sizes, $4^2 \times 33$, $6^2 \times 49$ and $8^2 \times 65$ for the Polyakov loop model and $24^2 \times 96$ for the Potts model. In each case we extracted the largest correlation length. We find that in the region of metastability the correlation length rises with increasing lattice size and shows approximate scaling with L. Outside that critical region we observe that ξ decreases for $\beta < \beta_c$, while it rises faster than L for $\beta > \beta_c$. This behavior is consistent with that expected for a first-order phase transition in models with global discrete symmetries.

The paper is organized as follows. In sect. 2 we present our results for thermodynamic quantities. Correlation length measurements are presented and discussed in sect. 3. A summary is given in sect. 4.

2. The models and their thermodynamics

2.1. THE MODELS

As already mentioned, interest in the 3-d three-state Potts model and the Polyakov loop model arises from the fact that they have the same global symmetry as the (3 + 1)-dimensional SU(3) gauge theory at finite temperature. In the strong coupling expansion [6, 7] of the lattice formulation of the latter, one can derive the Polyakov loop model by neglecting all the spacelike plaquettes in the gauge action. Then the remaining links can be integrated along the time direction at each spatial site of the lattice. This yields an expansion in characters of SU(3) which can be organized in strong coupling to give the partition function

$$Z_{\text{eff}} = \int \prod_i \mathrm{d}W_i \exp\left[2\beta \sum_{\langle ij \rangle} \mathrm{Re}\left(\mathrm{tr}\, W_i\, \mathrm{tr}\, W_j^{\dagger}\right)\right], \tag{2.1}$$

where β in this model can be related to the coupling g^{-2} of the SU(3) gauge theory [7]. The product is over sites of the three-dimensional lattice and the summation over pairs of nearest neighbours. The SU(3) matrix W_i appearing in the action is the Polyakov loop in the original gauge action and the measure is, as usual, the Haar measure on SU(3). Note that the Z_3 invariance of the original SU(3) gauge theory action has been preserved, and that the interaction is short-ranged and ferromag-

netic ($\beta > 0$). Within this approximation it is also possible to include next-nearest neighbour interactions etc.; they all turn out to lead to ferromagnetic couplings.

Since the field W_i appears in the action only in the form $\mathrm{tr}\, W_i$, we have the freedom of an independent gauge transformation at each lattice site

$$\mathrm{tr}\, W_i \mapsto \mathrm{tr}\left(g_i W_i g_i^\dagger\right),$$

where g_i is any element of SU(3). Through such transformations, we can always restrict $\mathrm{tr}\, W_i$ to the maximal abelian subgroup (U(1) × U(1)) of SU(3)

$$\mathrm{tr}\, W_i = \left(e^{i\theta_{i1}} + e^{i\theta_{i2}} + e^{i\theta_{i3}}\right) \qquad (\theta_{i3} = -\theta_{i1} - \theta_{i2}). \tag{2.2}$$

The integral over the rest of the group can then be performed analytically, leaving the measure

$$\sin^2\left(\frac{\theta_{i1} - \theta_{i2}}{2}\right)\sin^2\left(\frac{\theta_{i2} - \theta_{i3}}{2}\right)\sin^2\left(\frac{\theta_{i3} - \theta_{i1}}{2}\right) d\theta_{i1}\, d\theta_{i2}\, d\theta_{i3}\, \delta(\theta_{i1} + \theta_{i2} + \theta_{i3}). \tag{2.3}$$

The partition function can then be written in the form

$$Z_{\mathrm{eff}} = \int \left\{ \prod_i d\theta_{1i}\, d\theta_{2i} \right\} \exp\left[2\beta \sum_{\langle ij \rangle} T_{ij} + 2 \sum_i V_i \right], \tag{2.4}$$

where

$$T_{ij} = \left[(\cos\theta_{1i} + \cos\theta_{2i} + \cos\theta_{3i})(\cos\theta_{1j} + \cos\theta_{2j} + \cos\theta_{3j}) \right.$$
$$\left. + (\sin\theta_{1i} + \sin\theta_{2i} + \sin\theta_{3i})(\sin\theta_{1j} + \sin\theta_{2j} + \sin\theta_{3j}) \right],$$

$$V_i = \left[\log\left(\sin\left(\frac{\theta_{1i} - \theta_{2i}}{2} \right) \right) + \log\left(\sin\left(\frac{\theta_{2i} - \theta_{3i}}{2} \right) \right) + \log\left(\sin\left(\frac{\theta_{3i} - \theta_{1i}}{2} \right) \right) \right]$$

with $$\theta_3 = -(\theta_1 + \theta_2).$$

The index i varies over lattice sites, and $\langle ij \rangle$ indicates pairs of nearest neighbours. The two angles at each site vary between zero and 2π. This is the form of the action we use in our Monte Carlo.

The 3-d three-state Potts model can be thought of as a result of further thinning out of degrees of freedom from eq. (2.1) which are irrelevant to the global Z_3 symmetry. Its partition function can be written as

$$Z_{\mathrm{P}} = \sum_{\{s_i\}} \exp\left[2\beta \sum_{\langle ij \rangle} \mathrm{Re}(s_i s_j^*) \right], \tag{2.5}$$

where $s_j = \exp(2\pi ik/3)$ $(k = 0, 1, 2)$ are the spin variables. The above model has been studied in detail in ref. [13] on cubic lattices. Here we will extend those investigations to the cylindrical geometry with different boundary conditions.

2.2. THERMODYNAMIC QUANTITIES

For the Polyakov loop model we have extracted thermodynamic quantities from 4^3, 6^3, 8^3, and 10^3 lattices for β between 0.136 and 0.139, while for Potts model we employed a $24^2 \times 96$ lattice and studied the range $0.365 \leqslant \beta \leqslant 0.368$. In the latter case we compared the thermodynamics on cylindrical lattices with different boundary conditions with earlier results obtained on cubic lattices. In both cases we used a Metropolis algorithm. In the critical region we performed several million iterations for each size of the lattice. We present here our analyses for the order parameters and the energy densities of the models, the observation of co-existing phases near the pseudocritical coupling β_c^L, and the response functions C_V (specific heat) and χ (susceptibility).

2.2.1. The Polyakov loop model. We can identify the phase of the system under study from scatter plots of $\mathrm{tr}\, W$ or histograms of $\mathrm{Re}(\mathrm{tr}\, W)$, where W denotes the average of W_i over the whole lattice,

$$W = (1/V) \sum_i W_i . \tag{2.6}$$

At small β, $\mathrm{tr}\, W$ clusters around zero, and the histogram peaks there. We identify this as the disordered phase. At large values of β these distributions are peaked sharply away from zero. Values of $\mathrm{tr}\, W$ cluster around the three Z_3 symmetric points $W_0 e^{i\phi_j}$ where $\phi_1 = 0$, $\phi_2 = 2\pi/3$ and $\phi_3 = 4\pi/3$. The distribution of $\mathrm{Re}(\mathrm{tr}\, W)$, as a consequence, has two peaks at $-W_0/2$ and W_0, with $W_0 \simeq 1.3$. The phase with this characteristic is identified as the ordered phase. At β close to 0.137, we see strong evidence of metastability between the *ordered* and the *disordered* phases, showing up as a distinct three-peak structure in the histograms. This behaviour is shown in fig. 1. The middle peak corresponds to the disordered phase, and the two peaks to its left and right correspond to the ordered phase, with W taking values in the different Z_3 vacua. At a given value of β, near β_c, the system can exist with more or less equal probability in either phase. These peaks do not tend to merge, or disappear, on the larger lattices; on the contrary, they tend to become sharper and more pronounced. We thus do not see any tendency for the potential barrier to disappear in the large volume limit, which is indicative of a first-order transition.

In fig. 2, we show how the system flips between the ordered and disordered phases through a Monte Carlo run on a 10^3 lattice near the critical point. The (Monte Carlo) time during which the system stays in one of the two phases is seen to be much larger than time spent in transition. Also, we note that almost all flips occur between ordered and disordered phases, and very few flips are observed

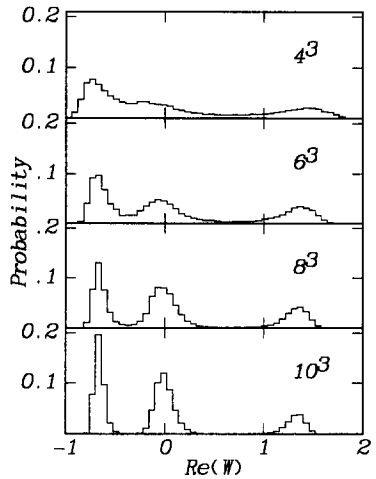

Fig. 1. Histogram of Re(tr W) for cubic lattices. Note that with increasing lattice size the peaks become narrower and better separated. The middle peak corresponds to the disordered phase. Shown are histograms for the 4^3 lattice $\beta = 0.1369$, for 6^3 at $\beta = 0.13705$, for 8^3 at $\beta = 0.1371$, and for 10^3 at $\beta = 0.13715$.

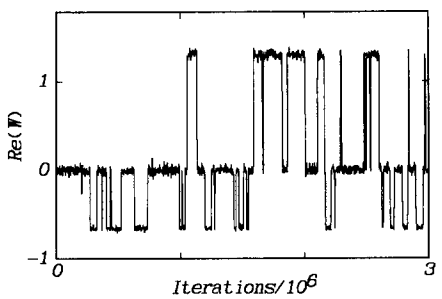

Fig. 2. The run time history for the quantity Re(tr W) on a 10^3 lattice at $\beta = 0.1372$.

between the different Z_3 vacua of the disordered phase. The barrier between the three minima of the broken phase is thus higher than the barrier which separates them from the disordered phase. The frequency of flips between ordered and disordered phases decreases rapidly with increasing lattice volume. On the 8^3 lattice, there are about 150 flips per 10^6 Monte Carlo sweeps at $\beta = 0.1371$. At the same β, on a 10^3 lattice, the rate falls to 20 per 10^6 sweeps.

Let us now discuss the behaviour of some thermodynamic observables. We have studied the energy density

$$\epsilon = (1/V)\left\langle 2 \sum_{\langle ij \rangle} T_{ij} \right\rangle, \tag{2.7}$$

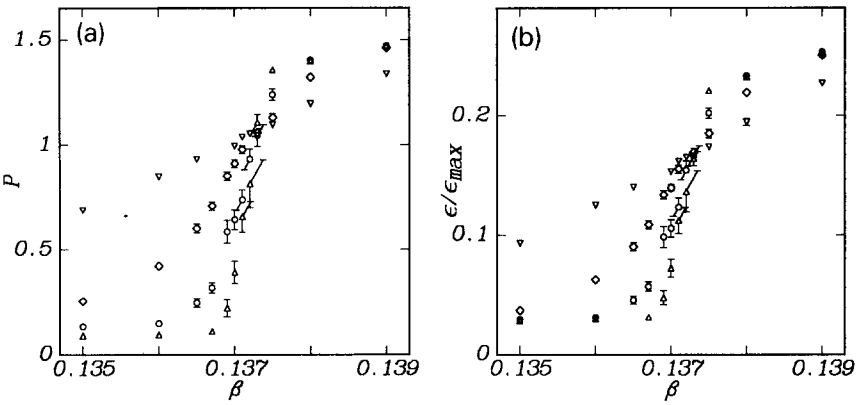

Fig. 3. (a) The order parameter P, and (b) the energy density ϵ as function of β on 4^3 (lower triangles), 6^3 (circles), 8^3 (diamonds) and 10^3 (upper triangles) lattices.

and the order parameter

$$P = \langle \mathrm{Abs}(\mathrm{tr}\, W) \rangle . \tag{2.8}$$

Note that P is not strictly an order parameter because the global Z_3 symmetry of the action does not constrain it to a zero value in the symmetric phase. Nevertheless, we observe that in the absence of an external Z_3 field, it averages statistically to a small value that is expected to scale inversely with the lattice volume.

The behaviour of P as a function of β on different lattices is shown in fig. 3. As can be seen, the sharpness of the transition increases as the lattice size is increased. Note that the asymptotic values of the order parameter are reached smoothly on all the different lattices. The lattice size dependence seems to be larger for $\beta < \beta_c$ than for $\beta > \beta_c$. In fig. 3, we also show the energy density which exhibits a similar behaviour.

The more rapid change of P and ϵ in the transition region is reflected in the increasing peaks of the corresponding response functions at β_c^L. We extract the specific heat

$$C_V = \frac{4\beta^2}{V}\left[\left\langle \left(\sum_{\langle ij \rangle} T_{ij} \right)^2 \right\rangle - \left\langle \sum_{\langle ij \rangle} T_{ij} \right\rangle^2 \right], \tag{2.9}$$

and the susceptibility

$$\chi = V\left(\langle \mathrm{Abs}(\mathrm{tr}\, W)^2 \rangle - \langle \mathrm{Abs}(\mathrm{tr}\, W) \rangle^2 \right). \tag{2.10}$$

These are shown in figs. 4 and 5. It can be seen that on successively larger lattices the peak grows higher and narrows rapidly. We would like to stress again that also

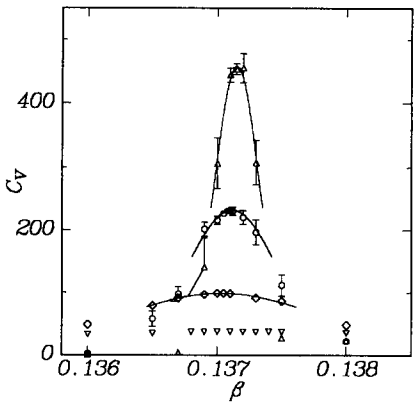

Fig. 4. Specific heat as a function of β on 4^3 (lower triangles), 6^3 (circles), 8^3 (diamonds) and 10^3 (upper triangles) lattices. The full lines show the gaussian fitted to the data and are extended over the range of the fits.

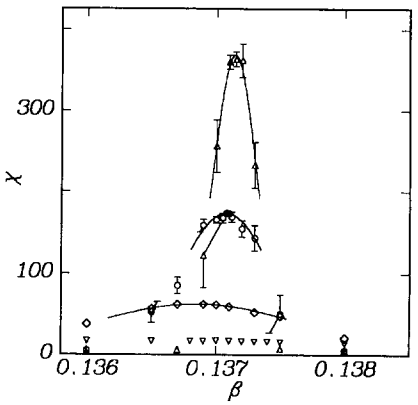

Fig. 5. Same as fig. 4 but for the susceptibility χ.

for a first-order phase transition the peaks in response functions are expected to diverge. In fact, for a first-order transition the divergence is expected to be fastest, i.e. proportional to V, while in a second-order transition the peak scales with a characteristic critical exponent L^y, with $y \leqslant d$. A finite size scaling analysis of this phenomenon should thus allow us to distinguish between a first- and second-order phase transition [11, 12].

We have checked this scaling behaviour in detail by fitting the region near the peak of each of these curves by a gaussian. The maxima of the curves are obtained from the fits. The fitted curves are displayed in figs. 4 and 5 as the full lines. The values at the peak for both C_V and χ are found to scale linearly with V. This is shown in fig. 6, where we also display the expectations for the peak values based on the relations

$$C_V^{\text{peak}}/V \simeq \beta_c^2 \left(\tfrac{1}{2}\Delta\epsilon\right)^2, \qquad \chi^{\text{peak}}/V \simeq \left(\tfrac{1}{2}\Delta P\right)^2. \tag{2.11}$$

Here $\Delta\epsilon$ and ΔP denote the discontinuity in the energy density and the order parameter, respectively. From the histograms for ϵ and P we obtain for the gap in these quantities at β_c.

$$\Delta\epsilon/\epsilon_{\max} = 0.182 \pm 0.009, \qquad \Delta P = 1.25 \pm 0.07. \tag{2.12}$$

It is interesting to note that the gap in the order parameter agrees well with that found in the 3-d Potts model [13]. Also in that case we have checked that the peaks in C_V and χ scale according to the relations given in eq. (2.11).

Let us finally discuss the scaling of the critical coupling β_c with lattice size. On a finite lattice the definition of the pseudocritical coupling is not unique. We explore three different definitions of β_c^L by using the peaks in the response functions C_V, χ

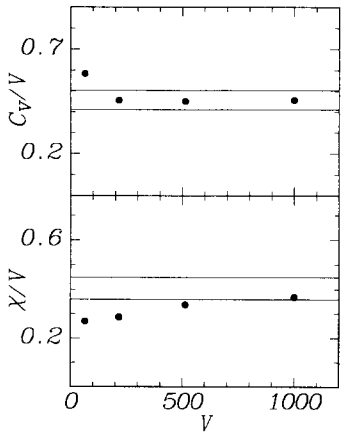

Fig. 6. The maxima of (a) C_V/V, and (b) χ/V, as obtained from the fits shown in figs. 4 and 5, plotted as a function of the lattice volume. The bands give upper and lower limits as obtained from eqs. (2.11) and (2.12).

TABLE 1
Pseudocritical coupling β_c^L on L^3 lattices as obtained from the three methods indicated

L	β_c^L		
	histogram	peak of χ	peak of C_V
6	0.1368 (1)	0.13685(2)	0.13703(3)
8	0.1371 (1)	0.13708(2)	0.13711(2)
10	0.13715(5)	0.13714(1)	0.13715(1)
∞	0.13721(5)	0.13722(2)	0.13718(2)

as well as the relative populations in the different phases seen in the critical region [13]. In all the cases β_c^L can be extracted from a gaussian fit to the data. The results of our analysis for β_c^L are given in table 1. β_c^∞ is obtained by assuming that the shift on a finite lattice scales inversely with volume $V = L^3$:

$$\beta_c^L = \beta_c^\infty + a/V. \tag{2.13}$$

We find that the bulk transition takes place at $\beta = 0.13720 \pm 0.00003$. A posteriori the agreement of various estimates for β_c^∞ in table 1 also implies that the shift exponent for the critical coupling is consistent with 3, the dimensionality of the lattice. This, together with the evidence presented above, supports the first-order nature of the transition in the Polyakov loop model. We note that our results are in good agreement with the mean field results for this model, which predict a first-order phase transition at $\beta_c = 0.134$ [7].

2.2.2. The Potts model. The thermodynamics of the Potts model on cubic lattices with periodic boundary conditions has been studied in detail in ref. [13]. Here we concentrate on the differences arising from the change of geometry and boundary conditions. In fig. 7 we show the energy density, ϵ, and the order parameter, S, on a $24^2 \times 96$ lattice with and without a cold wall*. For comparison we also display corresponding results on the 36^3 lattice from ref. [13]. This lattice has approximately the same volume as the $24^2 \times 96$ lattice. We note that the results obtained with the periodic boundary conditions seem to be independent of the geometry whereas the cold wall boundary conditions lead to large finite size effects in both shape and

* We use the same definitions for ϵ and S as in ref. [13].

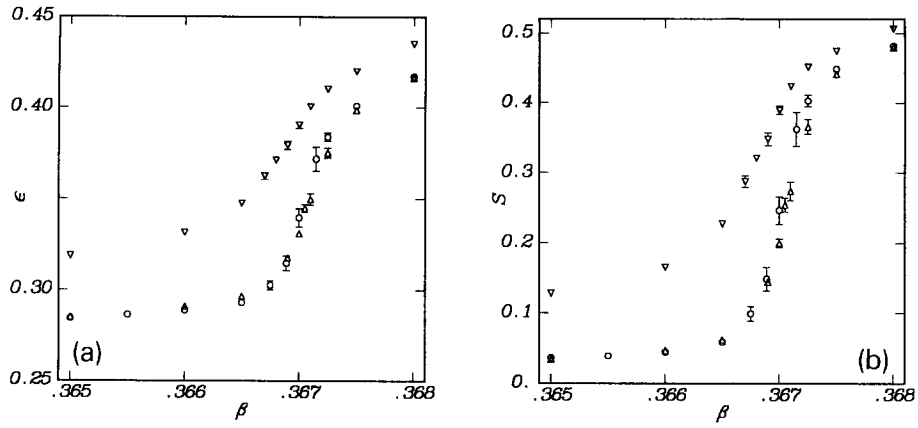

Fig. 7. (a) The energy density ϵ, and (b) the order parameter S, as a function of β for the 3-d three-state Potts model. Shown are results from simulations on 36^3 (open circles) and $24^2 \times 96$ (upper triangles) lattices with periodic boundary conditions and from a $24^2 \times 96$ lattice with a cold wall (lower triangles).

magnitude. These effects are expected to vanish as the longitudinal size of the lattice goes to infinity. However, our results show that a lattice with longitudinal size only a factor of 4 bigger than the transverse size is still far away from this ideal case.

3. Correlation length measurements

As is well known, on an infinite lattice the correlation length diverges at a second-order phase transition but remains finite at a first-order transition, thus providing a clear signal for the order of the transition. In terms of the mass $\mu(\beta)$, defined by the correlation function of a nonsinglet operator $O(z)$,

$$\langle O(z)O(0)\rangle \sim \mathrm{e}^{-\mu(\beta)z}, \qquad z \to \infty, \tag{3.1}$$

a first-order transition corresponds to a discontinuity at β_c. The mass $\mu(\beta)$ is finite for $\beta < \beta_c$ and zero for $\beta > \beta_c$. If the phase transition is of second order, there is no discontinuity at β_c but $\mu(\beta)$ decreases to zero continuously as $\beta \to \beta_c^-$. Note that $\mu(\beta)$ corresponds to the physical mass gap only for $\beta < \beta_c$. Above β_c, it merely reflects the non-vanishing expectation value of the operator $O(z)O(0)$, as $z \to \infty$, i.e. the appearance of a spontaneously broken phase. To extract the physical correlation length in the broken phase, where $\mu(\beta) = 0$, one has to study the connected correlation function $\langle O(z)O(0)\rangle - \langle O(0)\rangle^2$.

On a finite lattice, on the other hand, the distinction between first- and second-order behaviour is less clear-cut. For definiteness, let us consider correlations between zero-momentum operators $O(z)$ on a lattice length L_z in the z direction and of transverse size L^2, with $L_z \gg L$. In terms of the masses $\mu_0 < \mu_1 < \ldots$ on the

$L^2 \times \infty$ lattice, which are determined by the eigenvalues of the transfer matrix in the z direction, one can write

$$\langle O(z)O(0)\rangle = \sum_i A_i(L,\beta)(\exp[-\mu_i(L,\beta)z] + \exp[-\mu_i(L,\beta)(L_z - z)]) \tag{3.2}$$

for a lattice periodic in the z direction. From the discussion above, one expects that the mass gap $\mu_0(L,\beta)$ tends to a finite value (zero value) as $L \to \infty$ for fixed $\beta < \beta_c$ ($\beta > \beta_c$). For a large but finite value of L, μ_0 will therefore drop sharply but continuously close to β_c, irrespective of the order of the transition.

Knowledge of $\mu_0(L,\beta)$ will in the $L \to \infty$ limit provide us with the physical correlation length ξ for $\beta < \beta_c$. In order to determine ξ in the broken phase, one can exploit the fact that for sufficiently high β, $\mu_0 L_z \ll 1$ and the first term in eq. (3.2) becomes effectively a constant, corresponding to a non-vanishing term that needs to be subtracted to obtain the connected correlation function. Effectively, one can then estimate ξ from the large distance approximation

$$\langle O(z)O(0)\rangle = A\cosh\left(\xi^{-1}\left(\tfrac{1}{2}L_z - z\right)\right) + B, \qquad 0 \ll z \ll L_z. \tag{3.3}$$

In the critical region, where we expect $\mu_0 L_z \sim O(1)$, this is, however, not a good approximation to eq. (3.2). Since this is the region we are interested in, we prefer to discuss correlations in terms of the μ_i of eq. (3.2). The order of the transition is then signalled by the $L \to \infty$ behaviour of these masses, as discussed above.

A widely used method for correlation length measurements is the source method, which is expected to give a better signal to noise ratio than ordinary correlation function measurements. Following ref. [3], we use this method with a cold wall as a source. We fix all the field variables at $z = 0$ and $z = L_z$ to identify and measure the response function

$$C_w(z) = \mathrm{Re}\,\overline{W}(z), \tag{3.4}$$

with $\overline{W}(z)$ defined as the average of Polyakov loops in a transverse plane at distance z from the source:

$$\overline{W}(z) = (1/L^2)\sum_{x,y} \mathrm{tr}\, W(x,y,z). \tag{3.5}$$

From these measurements we extract local masses $\mu(z)$, defined by

$$\frac{\langle C_w(z)\rangle}{\langle C_w(z+1)\rangle} = \frac{\cosh[\mu(z)(L_z/2 - z)]}{\cosh[\mu(z)(L_z/2 - z - 1)]}. \tag{3.6}$$

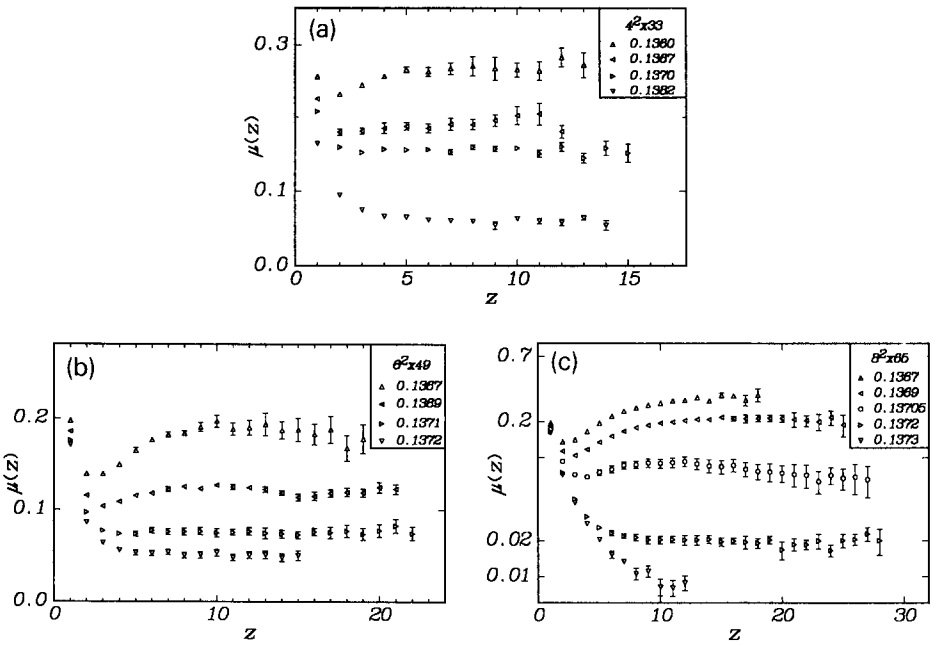

Fig. 8. Local masses $\mu(z)$, obtained with the source method, as a function of z at different β values for lattice sizes (a) $4^2 \times 33$, (b) $6^2 \times 49$ and (c) $8^2 \times 65$.

At intermediate distances $\mu(z)$ is an effective mass that gets contributions from all masses μ_i. At sufficiently large distances, however, it will be dominated by the lowest excitation μ_0. In order to check a possible sensitivity of our results to the choice of boundary conditions, we have also measured the correlation function

$$C_{\mathrm{pb}}(z) = \mathrm{Re}\big(\overline{W}(z)\overline{W}^{\dagger}(0)\big). \tag{3.7}$$

This we have done on periodic lattices of the same sizes at a number of different β values. For the analysis we follow the same procedures as above. A similar analysis has also been performed for the Potts model on a $24^2 \times 96$ lattice. In this case $\overline{W}$ defined in eq. (3.5) has to be replaced by an appropriate spin average as defined in ref. [13].

3.1. THE POLYAKOV LOOP MODEL

In figs. 8 and 9 we show $\mu(z)$ at several β values for the three lattice sizes $4^2 \times 33$, $6^2 \times 49$ and $8^2 \times 65$ obtained from $C_{\mathrm{w}}(z)$ and $C_{\mathrm{pb}}(z)$, respectively. The errors have been estimated by extracting $\mu(z)$ from four or eight subsamples (or blocks) of the data. The number of iterations used to determine $C_{\mathrm{w}}(z)$ at each β is

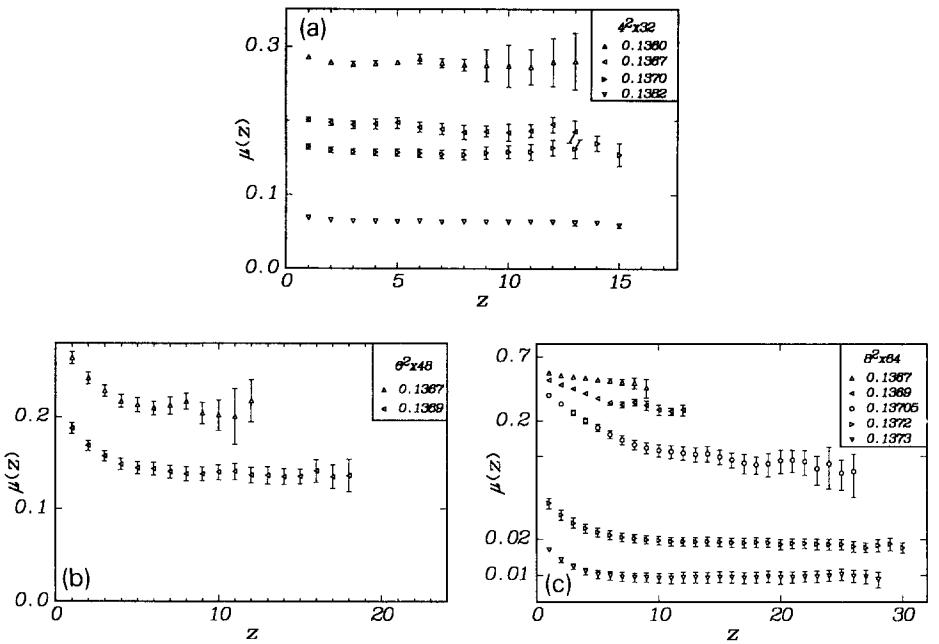

Fig. 9. Same as fig. 8 but with $\mu(z)$ obtained from the correlation function function C_{pb}. The lattice sizes are (a) $4^2 \times 32$, (b) $6^2 \times 48$ and (c) $8^2 \times 64$.

TABLE 2

Inverse correlation length μ as obtained from the source method on a $8^2 \times 65$ lattice. Data for $C_{\mathrm{w}}(z)$ (eq. 3.4), $d_{\min} \leqslant z \leqslant d_{\max}$, have been fitted to the expression eq. (3.8).

β	blocks	iterations	$d_{\min}$	$d_{\max}$	μ	χ^2	DOF
0.1360	40	0.5×10^6	11	16	0.4620(391)	5.40	4
0.1365	40	0.5×10^6	11	22	0.4027(167)	11.24	10
0.1367	75	3.0×10^6	15	24	0.3246(109)	10.42	8
0.1368	40	0.5×10^6	15	24	0.2772(154)	8.62	8
0.1369	75	3.2×10^6	17	30	0.2148(97)	12.10	12
0.1370	75	4.0×10^6	21	30	0.1314(108)	5.18	8
0.13705	50	3.0×10^6	21	30	0.0718(67)	11.67	8
0.1371	30	1.0×10^6	21	30	0.0528(73)	8.13	8
0.1372	75	4.0×10^6	21	32	0.0192(20)	18.06	10
0.1373	100	3.0×10^6	21	32	0.0080(18)	14.65	10

TABLE 3
Same as table 2 for the $6^2 \times 49$ lattice

β	blocks	iterations	$d_{\min} d_{\max}$	μ	χ^2	DOF	
0.1360	40	0.5×10^6	9	18	0.3589(155)	4.33	8
0.1365	40	0.5×10^6	11	18	0.2664(122)	5.57	6
0.1367	40	1.5×10^6	11	24	0.1860(61)	7.34	12
0.1368	40	0.5×10^6	11	24	0.1448(70)	9.28	12
0.1369	60	2.3×10^6	16	24	0.1171(34)	7.19	7
0.1370	40	1.0×10^6	16	24	0.0942(48)	3.86	7
0.13705	40	1.0×10^6	16	24	0.0826(58)	5.54	7
0.1371	40	1.5×10^6	16	24	0.0770(42)	3.23	7
0.1372	40	1.0×10^6	16	24	0.0481(39)	6.10	7
0.1374	40	1.0×10^6	16	24	0.0294(28)	2.41	7
0.1376	40	0.5×10^6	16	24	0.0132(44)	8.10	7

TABLE 4
Same as table 2 for the $4^2 \times 33$ lattice

β	blocks	iterations	$d_{\min}$	$d_{\max}$	μ	χ^2	DOF
0.1360	80	2.0×10^6	7	16	0.2681(54)	4.00	8
0.1365	40	0.5×10^6	7	16	0.2108(67)	10.72	8
0.1367	40	0.5×10^6	7	16	0.1931(60)	5.98	8
0.1368	40	0.5×10^6	7	16	0.1686(56)	16.11	8
0.1369	40	0.5×10^6	7	16	0.1605(64)	9.07	8
0.1370	80	2.0×10^6	9	16	0.1571(30)	7.87	6
0.13705	40	1.0×10^6	9	16	0.1513(37)	2.34	6
0.1371	40	1.0×10^6	9	16	0.1404(38)	1.70	6
0.1372	40	0.5×10^6	9	16	0.1308(58)	4.11	6
0.1374	40	0.5×10^6	9	16	0.1060(52)	2.36	6
0.1378	40	1.0×10^6	9	16	0.0764(32)	6.37	6
0.1382	40	1.5×10^6	9	16	0.0629(15)	9.12	6

at least 0.5×10^6 and up to 4.0×10^6 near the critical point on the largest lattice. Corresponding numbers for $C_{\mathrm{pb}}(z)$ are in general higher (see tables 2–5).

A constant value of $\mu(z)$ signals that the first term dominates in eq. (3.2) in that range of z. In figs. 8 and 9 this behaviour is observed in most of the cases and the mass gap can therefore be read off directly. Comparing these figures, we see that at small distances, the distance-dependent masses $\mu(z)$ are different in the two cases. This is to be expected since the corresponding coefficients A_i in eq. (3.2) are different. Due to the positivity of all A_i in the case of lattices with periodic boundary conditions, the large distance limit for the local masses is approached from above, whereas at least for $\beta < \beta_c$ it seems to approach the asymptotic value from below in the presence of a source. More importantly, we find that at large

TABLE 5
Inverse correlation length μ as obtained from a fit of the data for the correlation function $C_{pb}(z)$ (eq. (3.7)), $d_{min} \leq z \leq d_{max}$, to the expression eq. (3.8).

Size	β	blocks	iterations	d_{min}	d_{max}	μ	χ^2	DOF
64×8^2	0.1367	75	4.0×10^6	6	10	0.4398(203)	1.85	3
	0.1369	75	2.9×10^6	9	18	0.2615(312)	3.60	8
	0.13705	75	10.0×10^6	18	28	0.0904(248)	9.51	9
	0.1372	75	6.0×10^6	20	30	0.0184(16)	14.82	9
	0.1373	75	3.0×10^6	20	30	0.0089(7)	11.75	9
48×6^2	0.1367	50	1.6×10^6	10	16	0.2047(104)	7.88	5
	0.1369	50	1.6×10^6	12	20	0.1286(84)	5.82	7
32×4^2	0.1360	50	2.0×10^6	4	16	0.2774(41)	2.97	11
	0.1367	50	1.0×10^6	8	16	0.1859(64)	5.81	7
	0.1369	50	1.0×10^6	8	16	0.1663(57)	7.08	7
	0.1370	50	1.0×10^6	8	16	0.1543(43)	9.53	7
	0.1382	50	1.0×10^6	8	16	0.0638(23)	2.03	7

distances the two local masses seem to converge nicely to a common limit, thus suggesting that the same longest correlation length is measured. We have also extracted the mass gap from a global fit of our data for $C_w(z)$ and $C_{pb}(z)$ to the expression

$$f(z; A, \mu) = A \cosh\left(\mu\left(\tfrac{1}{2}L_z - z\right)\right), \qquad 0 \ll z \ll L_z. \tag{3.8}$$

Since measurements of the different $C(z)$'s are strongly correlated, especially in the critical region, we use for our fits a definition of χ^2 including off-diagonal terms. Following ref. [14], we define the best fit by minimizing

$$\chi^2 = \sum_{z_1, z_2} \left(\langle C(z_1)\rangle - f(z_1; A, \mu)\right) V^{-1}_{z_1 z_2} \left(\langle C(z_2)\rangle - f(z_2; A, \mu)\right). \tag{3.9}$$

After dividing the measurements into N separate blocks, we estimate the covariance matrix $V_{z_1 z_2}$ in eq. (3.7) as

$$V_{z_1 z_2} = \frac{1}{N-1}\left(\frac{1}{N}\sum_{k=1}^{N} C_k(z_1) C_k(z_2) - \langle C(z_1)\rangle \langle C(z_2)\rangle\right) \tag{3.10}$$

where $C_k(z)$ is the average over the kth block. For this to be a good estimate we need a large number of statistically independent blocks, i.e., the individual blocks should be large enough. The latter requirement is, of course, especially important in the presence of metastabilities. When choosing the block size, we checked that the diagonal elements of $V_{z_1 z_2}$ were reasonably N independent. The number of blocks N

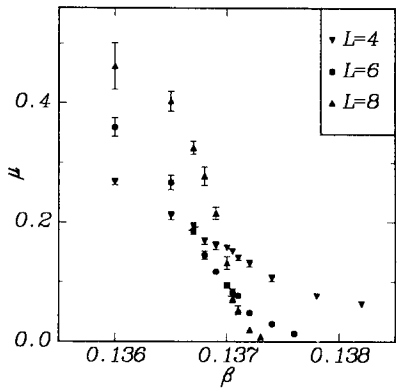

Fig. 10. Inverse correlation length μ as a function of β for different transverse sizes L.

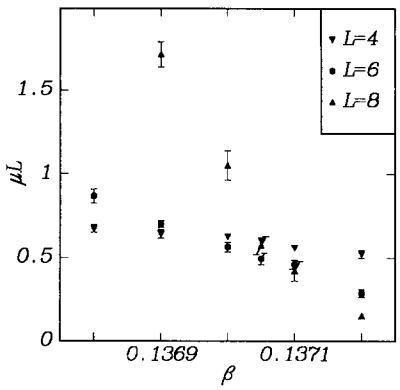

Fig. 11. The Fisher scaling variable μL as a function of β for different transverse sizes L.

we have used varies between 30 and 100, corresponding to block sizes of 10 000–130 000 iterations. Further details of the fits are given in tables 2–5. Errors quoted are defined as the region of parameter space over which χ^2 increases by one unit, assuming that this region is of quadratic shape. We note that the relative efficiency of the two different methods is β-dependent. In the disordered phase, we needed about three times more statistics for the correlation function on the largest lattice without a source than in the case with a cold wall to obtain similar statistical errors. In the ordered phase, on the other hand, the method without the source seems to be the most efficient one.

The values for the mass μ as given in tables 2–5 are in good agreement with estimates from the local masses. Comparing again the source method results (tables 2–4) with those obtained without a source (table 5), we find in general a very good agreement. We further note that the χ^2 per degree of freedom for the fits are in the range 0.25 to 2.0. This, together with an approximately constant long-distance behaviour of the local mass, we take as evidence that our values for μ are reasonable estimates of μ_0. Fig. 10 displays μ as a function of β for all the lattices sizes we studied. From this figure we see that the decrease of μ in the critical region becomes significantly sharper with increasing L. In addition we also find that outside the critical region μ increases (decreases) with increasing lattice size for $\beta < \beta_c$ ($\beta > \beta_c$). This suggests that a discontinuity develops in the infinite volume limit, as expected for a first-order transition.

In fig. 11 we show the Fisher scaling variable μL in the neighbourhood of the phase transition. We note from this figure that there exists a β value at which the Fisher scaling variable corresponding to different L's are roughly equal. This implies that at this β the correlation length scales linearly with L, which is the behaviour expected at β_c for a second-order phase transition. However, our results

TABLE 6
Next largest correlation length for $L = 8$ as obtained from fits of the data indicated in the second column. Details of the fits are given in the text.

β	data	blocks	$d_{\min}$	$d_{\max}$	μ_0	μ_1	χ^2	DOF
0.1372	C_{pb}	50	4	14	0.0193(16)	0.4288(189)	6.82	7
0.1373	C_{pb}	75	2	12	0.0095(5)	0.6461(243)	8.27	7
0.1375	C_w	133	3	12	–	0.7148(617)	5.70	7

also show that, at least with a moderate number of different L's available, this behaviour cannot be used to determine the order of the transition. If the transition were of second order, then the finite size scaling behaviour of the Fisher scaling variable would be given by

$$\mu L = a + bL^{1/\nu}\left(\beta - \beta_c^L\right) \tag{3.11}$$

for β close to β_c^L. It is evident from the data shown in fig. 11 (see also fig. 15 for the Potts model) that the validity regime of this linear relation shrinks with increasing lattice size; for the numerical analysis a quadratic fit thus becomes necessary. We have fitted the Fisher variable on all three lattice sizes to a polynomial in $(\beta - \beta_c^L)$. For the two smaller lattices a linear form suffices. The resulting fits, when investigated close to β_c^L are consistent with $\nu = \frac{1}{3}$*. The volume dependence of our data for $\beta < \beta_c$ (but $\beta_c - \beta$ not too small) is also consistent with the form

$$\xi = a + b/L^2(\beta - \beta_c), \tag{3.12}$$

suggested [16] for a first-order transition on the basis of an effective potential model neglecting instanton effects. Fits to this form suggest that on a lattice infinite in all directions $\xi(\beta \to \beta_c^-) \approx 2$.

All the results above refer to the mass gap μ_0. At high β values on the largest lattice we have also calculated the next largest correlation length (see table 6). At $\beta = 0.1372$ and 0.1373 this was done by a two-mass, i.e. four-parameter, fit of the data for $C_{pb}(z)$. As seen from table 6, the χ^2 per degree of freedom for the fits are close to one and we further note that the values obtained for μ_0 are in nice agreement with our previous results. Fits to the simplified three-parameter expression eq. (3.3) are in this β region less well behaved. At $\beta = 0.1375$, on the other

* A similar analysis of the Fisher scaling variable has recently been performed for the SU(3) transition [15]. Qualitatively their results on the Fisher variable are very similar to ours. They analyse their data using the linear form given in eq. (3.11). On their largest lattices they find that ν does not agree with $\frac{1}{3}$. We note, however, that with increasing lattice size the scaling region, in which eq. (3.11) is valid, decreases rapidly. We find from our analysis that using this linear relation in a too large β interval leads to an overestimate of ν on larger lattices. This may be the reason why their estimates for ν are consistent with $\frac{1}{3}$ on small lattices only.

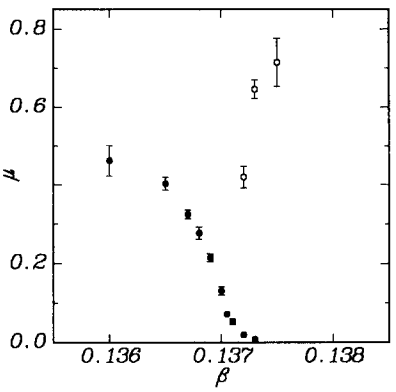

Fig. 12. μ_0 (filled circles) and μ_1 (open circles) as a function of β for $L = 8$.

hand, μ_0 is very small and it is possible to extract the next largest correlation length from the three parameter fit. In fig. 12, we have collected our results for μ_1 as well as μ_0 for $L = 8$. This figure suggests that the physical correlation length remains small also on the high β side of the transition. We estimate it to be of the order of two lattice spacings at β_c. We also attempted to determine the physical correlation length according to the prescription suggested in ref. [17]. We find, however, that results are strongly dependent on the parameters of the prescription, such as the criterion used to separate the two coexisting phases or to subtract the disconnected part in the correlation functions.

3.2. THE POTTS MODEL

Figs. 13 and 14 display the local masses $\mu(z)$ for the Potts model on a $24^2 \times 96$ lattice with and without a cold wall respectively. They exhibit the same behaviour as those for the Polyakov loop model, namely, in the absence of a wall they approach their asymptotic value from above for all β and the asymptotic values themselves are independent of the boundary conditions. Note that the statistics for both the figures are comparable and so are roughly the ranges from which an asymptotic value can be extracted in either case. We therefore do not see any particular advantage which selects one of them in this case. The resultant asymptotic masses are more or less the same as those obtained on a 36^3 lattice: while they do differ somewhat for $\beta \ll \beta_c$, near β_c they coincide. In fig. 15, we plot the Fisher scaling variable obtained from the data in ref. [13]. Again, we can find a β where values of μL corresponding to several different L's are approximately equal. Again an estimate of ν on the basis of eq. (3.11) is consistent with $\frac{1}{3}$. However, on the larger lattices the scaling region is very small and a better coverage of this region would be needed for a systematic analysis of ν based on the correlation length.

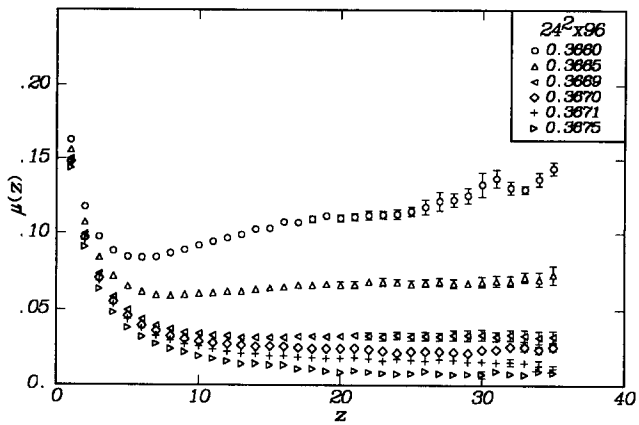

Fig. 13. Local masses $\mu(z)$ as a function of z obtained with the source method on a $24^2 \times 96$ lattice size for the Potts model at different β values.

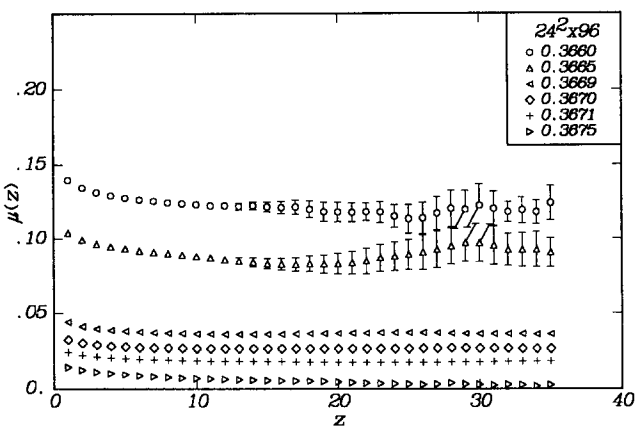

Fig. 14. Same as fig. 13 but without a source.

4. Discussion and conclusions

In this article we have studied in detail the phase transition in an effective three-dimensional model for the Polyakov loop with ferromagnetic coupling, which is related to finite temperature SU(3) gauge theory. We have also extended the study of the three-dimensional three-state Potts model, which was performed in ref. [13]. Both models have the same global Z_3-symmetry as the SU(3) gauge theory, and a phase transition to a phase where this symmetry is spontaneously broken.

In order to determine the order of the phase transition, one may choose to study global quantities like the order parameter and the energy density, or the behaviour

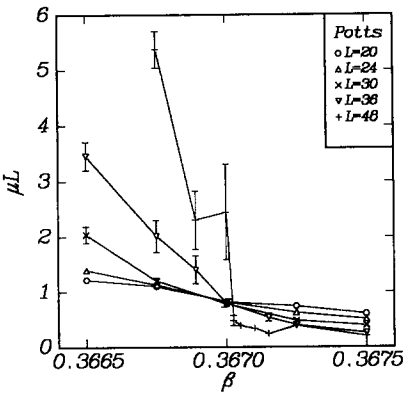

Fig. 15. The Fisher scaling variable for the 3-d three-state Potts model as a function of β. The data are taken from the correlation length measurements on periodic L^3 lattices presented in ref. [13].

of the correlation length near the transition. We have found that in both models the finite size scaling analysis of the global quantities gives clear evidence for a first-order phase transition. The analysis of the correlation length turns out to be more subtle.

In particular, we describe, in this article, measurements in the Polyakov loop model of the probability distributions of the order parameter, its absolute value, and of the energy density (average action). The measurements were performed on lattices of size 4^3, 6^3, 8^3 and 10^3. For all quantities we find, at the transition point, well-separated peaks, one corresponding to the disordered phase and the other (in the case of the order parameter, and three others) to the ordered phase. The separation of the peaks is independent of the lattice size. This corresponds to a finite size dependence of the corresponding response functions (specific heat and susceptibility), where the maximum of these quantities is proportional to the volume. This is in contrast with what is expected for a second-order transition, where the probability distribution shrinks, does not show well-separated peaks, and the maxima of the response functions accordingly grows slower than the volume with a rate given by the critical indices.

For the Potts model, we have data on correlations between spins on cubic lattices with size up to 48^3 and on $24^2 \times 96$. For the latter we also explore the influence of a cold wall. The corresponding data in the Polyakov loop model have been collected mainly by using the response to a cold wall. In some cases we have made runs with periodic boundary conditions, measuring the correlation function. For the Polyakov loop model we find that below β_c the source method is the more efficient one. Above β_c, on the other hand, the method without the source becomes preferable, both for the longest and the next-longest correlation length. In the Potts model no such clear differences are observed.

For the interpretation of the unsubtracted correlation function that we measure, it is important to note that in the ordered phase, in the infinite volume limit, the largest correlation length is infinite. This corresponds to the constant which should be subtracted in this phase. On a finite lattice, or a lattice finite in the two transverse directions, this correlation length is finite, but exponentially large in this phase, because of the tunnelling between the Z_3 vacua. In the transition region, the behaviour is more complicated. In the infinite volume limit, one expects a discontinuity in the correlation functions for a first-order phase transition, while for a second-order phase transition the correlation length goes continuously to infinity when the phase transition is approached from the disordered phase. On a finite lattice there is, of course, no discontinuity. Thus the difference between these two cases is given only by the finite size scaling behaviour.

We find, in fact, a value of β where the correlation length scales like L, the transverse dimension of the lattice, on our three lattices. We do not, however, consider this to be evidence for a second-order phase transition. Our data are reasonably well described in the disordered phase to be a universal function of $L^2(\beta - \beta_c)$ in a form expected for a first-order phase transition. Close to the transition, a Fisher finite size scaling analysis shows that our data are consistent with a critical exponent $\nu = \frac{1}{3}$. This corresponds to a leading order β dependence of ξ through $L^2(\beta - \beta_c)$. For a first-order phase transition one expects $\alpha = 1$, $\gamma = 1$ and $\nu = 1/d$ [11]. These exponents are in good agreement with the scaling behaviour seen in our data for the Polyakov loop model, both for the global quantities and for the correlation length. The measurements of the correlation length necessary for the finite size scaling analysis are, however, considerably more time-consuming than for the global quantities.

Finally, trying to separate the physical correlation length in the ordered phase from the tunnelling correlation length leads, in the Polyakov loop model, to a quite small value $\xi = 2$. This is also what results from the analysis in the disordered phase. For the Potts model the corresponding correlation length $\xi \approx 10$ [13]. A posteriori, we find that we have used lattices considerably larger than the physical correlation length. We thus conclude that the phase transition for both models is first-order. From a strong-coupling analysis one would expect also the next-nearest neighbour interactions in the Polyakov loop model to be ferromagnetic, and not to change the nature of the phase transition, but making the correlation length longer.

On the methodological side, we conclude from our experience with these models that the finite size scaling behaviour of the global quantities seems to be easier to analyse than the correlation length. Neither a long correlation length, nor its scaling behaviour at one value of β seem to be sufficient to ascertain the order of the phase transition. A very careful simultaneous finite size scaling analysis of these quantities seems to be necessary to determine the order of the phase transition in SU(3) and related Z_3-symmetric models.

We would like to thank the Deutsche Forschungsgemeinschaft for financial

support under contract Pe 340/1-2. We are very grateful to HLRZ, Jülich and CERN for the computer time necessary for this project. One of us (B.P.) thanks A. Billoire, R. Lacaze, E. Marinari, A. Morel and in particular J. Zinn-Justin for discussions and the Stimulation project of the European community for financial support.

References

[1] F. Karsch, Z. Phys. C (Particles and Fields) 38 (1988) 147
[2] F.R. Brown, N.H. Christ, Y. Deng, M. Gao and T.J. Woch, Phys. Rev. Lett. 61 (1988) 2058
[3] P. Bacilieri et al., Phys. Rev. Lett. 61 (1988) 1545
[4] P. Bacilieri et al., Nucl. Phys. B318 (1989) 553
[5] L.G. Yaffe and B. Svetitsky, Phys. Rev. D26 (1982) 963; Nucl. Phys. B210 (1982) 423
[6] J. Polónyi and K. Szlachányi, Phys. Lett. B110 (1982) 395
[7] F. Green and F. Karsch, Nucl. Phys. B238 (1984) 297
[8] M. Okawa, Phys. Rev. Lett. 60 (1988) 1805
[9] F.Y. Wu, Rev. Mod. Phys. 54 (1982) 235
[10] L.A. Fernández, E. Marinari, G. Parisi, S. Roncolini and A. Tarancón, Phys. Lett. B217 (1989) 309
[11] M.E. Fisher and A.N. Berker, Phys. Rev. B26 (1982) 2507
[12] M.N. Barber, *in* Phase transitions and critical phenomena, Vol. 8, ed. C. Domb and J.L. Lebowitz (Academic Press, New York, 1983) p. 145
[13] R.V. Gavai, F. Karsch and B. Petersson, Nucl. Phys. B322 (1989) 738
[14] T.A. DeGrand and C.E. DeTar, Phys. Rev. D34 (1986) 2469;
S. Gottlieb, W. Liu, R.L. Renken, R.L. Sugar and D. Toussaint, Phys. Rev. D38 (1988) 2245
[15] B.A. Berg, R. Villanova and C. Vohwinkel, Phys. Rev. Lett. 62 (1989) 2433
[16] E. Brézin and J. Zinn-Justin, Nucl. Phys. B257 [FS14] (1985) 867;
J. Zinn-Justin, private communication
[17] M. Fukugita and M. Okawa, Kyoto University preprint, RIFP-790 (1989)